Synthesis, Aggregation, and Adsorption Phenomena of Shape-Persistent Macrocycles with Extraannular Polyalkyl Substituents

Sigurd Höger,*,§ Klaus Bonrad,§ Ahmed Mourran,*,‡ Uwe Beginn,‡ and Martin Möller‡

Contribution from the Max Planck Institute for Polymer Research, Ackermannweg 10, 55128 Mainz, Germany, and Organische Chemie III/Makromolekulare Chemie, Universität Ulm, D-89069 Ulm, Germany

Received November 16, 2000

Abstract: The synthesis of shape-persistent macrocycles based on the phenyl-ethynyl backbone containing various extraannular alkyl side chains is described. Although compound solubility increases with increasing size of the side groups, decreasing the solvent polarity induces aggregation of the rings by nonspecific interactions. This was investigated by proton NMR spectroscopy. The magnitude of aggregation can be varied by using solvent mixtures of different hexane content, supporting the model of a solvophobic effect. From 1,2,4-trichlorobenzene solution the macrocycle **1c** adsorbs at the surface of highly oriented pyrolitic graphite (HOPG). The two-dimensional order of the structure was investigated by scanning tunneling microscopy (STM) revealing the formation of a two-dimensional lattice of $p1_2mm$ symmetry with lattice parameters $A = 3.6$ nm, $B = 5.7$ nm, and $\Gamma = 74°$.

Introduction

One important objective in supramolecular chemistry is the preparation of molecules which organize into well-defined superstructures.[1] The possibility to control the organization by defined structure variations helps to understand the important forces and geometrical requirements necessary for molecular self-assembly. Moreover, these superstructures may act as templates for the arrangement of substances whose organization parameters are even more difficult to control, they may facilitate epitaxial or topographic organization.

Macrocyclic compounds and their aggregation phenomena have attained increasing attention over the past years.[2] Based on Chandrasekhar's pioneering work on columnar mesophases of discotic (disklike) molecules, rings with a defined internal void (shape-persistent macrocycles) were examined as valuable candidates for the formation of hollow columns.[3] One could envision that the arrangement of the molecules in an axial stack would produce a molecular tube that, if functionalized appropriately, may give rise to ion channels, micro reaction chambers or functionalized rodlike micellar aggregates.

The strength of the attractive forces between the single units of the stack can vary over a broad range. For example, multiple hydrogen bonds in cyclopeptides or cyclosaccharides lead to large association constants and, even at low concentrations, lead to the formation of extended structures.[4] Weaker forces, like $\pi-\pi$ interactions, have been used to aggregate phenyl-ethynyl or phenyl-butadienyl macrocycles.[5] In these cases the occurrence of aggregation strongly relies on the electronic structure of the molecules; only macrocycles with electron-deficient core structures show the behavior of self-aggregation.[6]

During our work on the synthesis and the adaptable behavior of shape-persistent macrocycles we also became interested in the organization of these molecules into structures of higher dimensionality.[7] As we have shown in our previous work, the synthesis of functionalized structures can be performed in good to high yields by the oxidative coupling of rather rigid phenyl-ethynyl oligomers containing ethynyl end groups.[2b,8] Understanding how these molecules can be organized in a predictable way will provide the basis for obtaining defined arrangements of their functional groups in one or more dimensions.

* Corresponding author. Fax: (+49) 6131-379 100. E-mail: hoeger@mpip-mainz.mpg.de.

§ Max Planck Institute for Polymer Research.

‡ University of Ulm.

(1) (a) Lehn, J.-M. *Supramolecular Chemistry*; VCH: Weinheim, 1995. (b) Schneider, H.-J.; Yatsimirsky, A. *Principles and Methods in Supramolecular Chemistry*, VCH: Weinheim, 2000. (c) Fuhrhop, J.-H.; Köning, J. *Membranes and Molecular Assemblies: The Synkinetic Approach*; The Royal Society of Chemistry: Cambridge, 1994.

(2) Reviews about shape-persistent macrocycles: (a) Moore, J. S. *Acc. Chem. Res.* **1997**, *30*, 402. (b) Höger, S. *J. Polym. Sci., Part A*: *Polym. Chem.* **1999**, *37*, 2685. (c) Haley, M. M.; Pak, J. J.; Brand, S. C. *Top. Curr. Chem.* **1999**, *201*, 81.

(3) (a) Chandrasekhar, S.; Sadashiva, B. K.; Suresh, K. A. *Pramana* **1977**, *7*, 471. (b) Mindyuk, O. Y.; Stetzer, M. R.; Heiney, P. A.; Nelson, J. C.; Moore, J. S. *Adv. Mater.* **1998**, *10*, 1363. (c) Lehn, J.-M.; Malthête, J.; Levelut, A. M.; *J. Chem. Soc., Chem. Commun*. **1985**, 1794. (d) van Nostrum, C. F. *Adv. Mater.* **1996**, *8*, 1027.

(4) (a) Ghadiri, M. R.; Kobayashi, K.; Granja, J. R.; Chadha, R. K.; McRee, D. E. *Angew. Chem.* **1995**, *107*, 76.; *Angew. Chem., Int. Ed. Engl.* **1995**, *34*, 3. (b) Clark, T. D.; Ghadiri, M. R. *J. Am. Chem. Soc.* **1995**, *117*, 12364. (c) Gattuso, G.; Menzer, S.; Nepogodiev, S. A.; Stoddart, J. F.; Williams, D. J. *Angew. Chem.* **1997**, *109*, 1615; *Angew. Chem., Int. Ed. Engl.* **1997**, *36*, 1451.

(5) (a) Zhang, J.; Moore, J. S. *J. Am. Chem. Soc.* **1992**, *114*, 9701. (b) Shetty, A. S.; Zhang, J.; Moore, J. S. *J. Am. Chem. Soc.* **1996**, *118*, 1019. (c) Tobe, Y.; Utsumi, N.; Kawabata, K.; Naemura, K. *Tetrahedron Lett.* **1996**, *37*, 9325. (d) Tobe, Y.; Utsumi, N.; Nagano, A.; Naemura, K. *Angew. Chem.* **1998**, *111*, 1347; *Angew. Chem., Int. Ed. Engl.* **1998**, *37*, 1285. (e) Tobe, Y.; Nagano, A.; Kawabata, K.; Sonoda, M.; Naemura, K. *Org. Lett.* **2000**, *2*, 3265.

(6) Independently, the solvophobic π-stacking of phenylene ethynylene macrocycles and oligomers has been reported by others: (a) Tanikawa, S.; Moore, J. S. *Polym. Prepr. (Am. Chem. Soc., Div. Polym. Chem.)* **1999**, *40* (2), 169. (b) Lahiri, S.; Thompson, J. L.; Moore, J. S. *J. Am. Chem. Soc.* **2000**, *122*, 11315.

(7) (a) Höger, S.; Enkelmann,V. *Angew. Chem.* **1995**, *107*, 2917; *Angew. Chem., Int. Ed. Engl.* **1995**, *34*, 2713. (b) Morrison, D. L.; Höger, S. *J. Chem. Soc., Chem. Commun*. **1996**, 2313.

(8) Höger, S.; Meckenstock, A.-D.; Müller, S. *Chem. Eur. J.* **1998**, *4*, 2421.

10.1021/ja003990x CCC: $20.00
Published on Web 05/22/2001

Scheme 1[a]

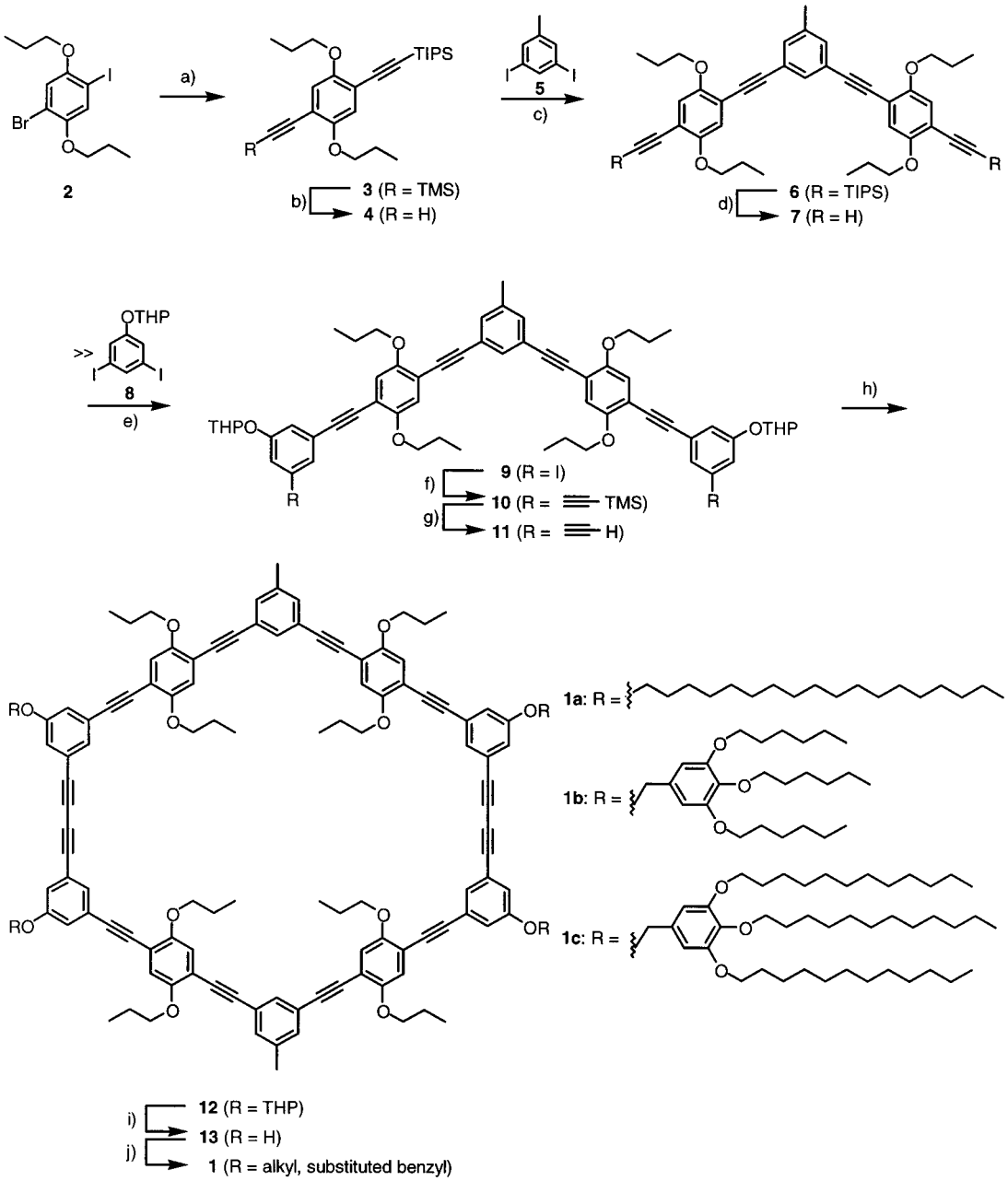

[a] Reagents and conditions: (a) i: TIPS acetylene, Pd(0) (cat.), Cu(I) (cat.), piperidine; ii: TMS acetylene, 84%; (b) K_2CO_3, MeOH, THF, 94%; (c), Pd(0) (cat.), Cu(I) (cat.), piperidine, 86%; (d) Bu_4NF, THF, 94%; (e) Pd(0) (cat.), Cu(I) (cat.), piperidine, 64%; (f) TMS acetylene, Pd(0) (cat.), Cu(I) (cat.), piperidine, 91%; (g) K_2CO_3, MeOH, THF, quant.; (h) CuCl, $CuCl_2$, pyridine, 48%; (i) *p*-TsOH, MeOH, $CHCl_3$, 98%; (j) alkyl halide, K_2CO_3, DMF, 14−48%.

Target structures for our investigation of the influence of different extraannular alkyl side groups on the melting and solubility properties of large rigid rings are compounds **1a**−**c** (Scheme 1).

They are based on a noncollapsible molecular backbone having a lumen of about 2 nm. The internal void of the rings is large enough to incorporate functional groups in a convergent arrangement,[9] and therefore these compounds serve as useful models for the purpose described above. Each ring contains eight propyloxy units and two methyl groups which ensure sufficient solubility of all intermediate compounds. In addition, the methyl groups simplify the proton NMR spectra in the aromatic region. This will be important if concentration-dependent NMR spectra are used to determine the association constants of these compounds. Per macrocycle, four phenol ether groups are pointing to the outside and act as connectors for the extraannular alkyl groups.

(9) Höger, S.; Meckenstock, A.-D. *Chem. Eur. J.* **1999**, *5*, 1686.

Results and Discussions

Synthesis. As shown in Scheme 1, the Glaser coupling of the bisacetylenes **11** was used for the cyclization reaction. However, two synthetic strategies to prepare **1** were considered. In the first strategy considered, the phenol corner pieces with the corresponding alkyl substituents could be joined prior to the ring formation. In this case a quadruple coupling reaction could be avoided, which may decrease the product yield. In the second strategy, the phenol macrocycle is formed first (via oxidative coupling of the tetrahydropyranyl (THP)-protected half

rings), followed by its derivatization with the alkyl groups. By using the second strategy the cyclization reaction had to be optimized only once. Furthermore, the second strategy was chosen because the R_f values of the cyclic dimers and the higher oligomers and polymers are often similar, making the product purification troublesome in cases where purification by recrystallization or reprecipitation is not possible.

The formation of the bisacetylenes was performed by a bidirectional synthesis starting from the toluoyl corner piece **5** (Scheme 1). Although the convergent-type synthesis of the bisacetylenes **11** starting from a protected phenol ether corner piece similar to **8** might have some advantages,[8] the required starting materials are not as easily available as in the procedure outlined here.

2-Bromo-5-iodo-1,4-dipropyloxybenzene **2**[10] was treated with 1.1 equiv of triisopropylsilyl (TIPS) acetylene at room temperature, and an additional 2 days at 55 °C. Subsequently, an excess of trimethylsilyl (TMS) acetylene (2 equiv) was added, and the mixture was stirred for an additional 2 days at the same temperature before workup. Deprotection of the TMS group of this coupling product (**3**) was performed by stirring with potassium carbonate in methanol/THF (1:1) overnight. Palladium-catalyzed coupling of **4** with 3,5-diiodotoluene (**5**), and desilylation of **6** by reaction with Bu_4NF gave **7**.

Protected 3-bromo-5-iodo-phenol, necessary for the selective coupling using the bromo-iodo strategy, is only available by a time-consuming multistep reaction starting from trinitrotoluene.[11] We therefore explored the possibility to use the much more available THP-protected 3,5-diiodophenol **8** in an excess reaction.[12] Reaction of a 6-fold excess of **8** with **7** afforded the diiodo compound **9** in 64% yield after chromatography. The excess of **8** was almost completely recovered. Palladium-catalyzed coupling of **9** with TMS acetylene gave **10**, from which the TMS groups were removed with potassium carbonate in THF/methanol. $CuCl/CuCl_2$-promoted coupling of the half ring **11** was performed under pseudo-high dilution conditions at 60 °C and gave the ring **12** in 45−50% yield. Mentioned previously, this temperature is a compromise between the increased coupling rate favoring the dimer formation and the decreased product stability at elevated temperatures.[13] Acid-catalyzed deprotection of the THP groups generated the tetraphenol **13** in quantitative yield.

We investigated three different extraannular alkyl side groups, which are either commercially available or were prepared.[14] Attachment of the side groups was accomplished by potassium carbonate-catalyzed reaction of **13** with an excess of the corresponding alkyl halide at 60 °C in DMF. The progress of the alkylation could be monitored by proton NMR spectroscopy (see Supporting Information). The proton signals from the phenolic parts of the ring shifted downfield after the alkylation, which was complete after 3−4 days. Purification of the rings was performed by repeated column chromatography. The low yield of **1a** was attributed to its restricted solubility, which complicated workup and purification.

All macrocycles **1** are slightly yellow solids. **1a** has a low solubility in common organic solvents (<1 mg ml^{-1}) and a melting point of about 220−222 °C. Investigations under the polarizing microscope gave no indications for the occurrence of a liquid crystalline (LC) phase.[15] Replacement of the four linear C18-chains by 12 C6-chains does not change the melting point dramatically, **1b** still has a melting point slightly above 200 °C. A meta-stable liquid crystalline phase was observed when the sample was quenched (15−20 °C/min), but the texture was fast superimposed by the formation of spherolites.[16] If the ratio of alkyl chains to the rigid backbone is increased, as in **1c**, the melting point decreased to 122−126 °C. Even so, a LC-phase was not observed. All of these observations are consistent with the notion that the large internal void of the rings hinders the formation of a stable LC-phase.[15]

Aggregation. Macrocycle **1a** is only moderately soluble in common organic solvents; whereas, **1b** and **1c** are readily soluble in THF and in aromatic and chlorinated solvents. The proton NMR data in these solvents are concentration-independent, giving no indications for the presence of any aggregation phenomena. However, it has been reported earlier that the aggregation constant of shape-persistent macrocycles is solvent-dependent, and solvophobic interactions are also responsible for the aggregation of self-assembled disk-shaped molecules.[5] Although in the case described here, the ratio of the aromatic backbone to the total surface of the molecule is much smaller (due to the size of the rings and their large internal void), we assumed that the aggregation of the macrocycles might be induced by adding a solvent which solubilizes the peripheric alkyl side chains and acts as a nonsolvent for the rigid macrocyclic core of the molecule. Indeed, the proton NMR spectra in the aromatic region of a solution of **1c** in a mixture of dichloromethane/*n*-hexane show a strong concentration dependence that increases as the proportion of the nonpolar solvent increases. All proton NMR signals remained distinct, and only a single set of signals was detected, indicating that aggregate formation and dissociation occurred rapidly on the NMR time scale. The aggregation constants were determined by measuring concentration-dependent chemical shifts of the aromatic protons of the macrocycle. Analysis of the data was performed under the assumption that the monomer−dimer equilibrium is the predominant process in solution.[17] Whereas macrocycle **1c** shows no aggregation in pure CD_2Cl_2, solvophobic interactions lead to an aggregation with a dimerization constant of $130 \pm 30\ M^{-1}$ in CD_2Cl_2/hexane-d_{14} (1:3 at 25 °C). A further polarity decrease of the solvent system by increasing the volume fraction of hexane increases the dimerization constant to $790 \pm 180\ M^{-1}$ (in CD_2Cl_2/hexane-d_{14} (1:6) at 25 °C). These data indicate that aggregation of the rings can be enforced by the addition of a solvent that acts as a good solvent for the alkyl chains and a poor solvent for the core (solvopho-

(10) Höger, S.; Bonrad, K.; Schäfer, G.; Enkelmann, V. *Z. Naturforsch.* **1998**, *53b*, 960. The formation of **3** also has been described by starting from 2,5-diiodo dipropyloxybenzene: Yu, C. J.; Chong, Y.; Kayyem, J. F.; Gozin, M. *J. Org. Chem.* **1999**, *64*, 2070. Opposite to our synthesis, a two-step reaction was used involving a statistical coupling reaction, which diminished the product yield.

(11) Hodgson, H. H.; Winall, J. S. *J. Chem. Soc.* **1926**, 2079.

(12) 3,5-Diiodo phenol was prepared by a modified literature procedure. Details on the synthesis are reported in the Supporting Information.

(13) Höger, S.; Bonrad, K.; Karcher, L.; Meckenstock, A.-D. *J. Org. Chem.* **2000**, *65*, 1588.

(14) Balagurusamy, V. S. K.; Ungar, G.; Percec, V.; Johansson, G. *J. Am. Chem. Soc.* **1997**, *119*, 1539.

(15) Höger, S.; Enkelmann, V.; Bonrad, K.; Tschierske, C. *Angew. Chem.* **2000**, *112*, 2356; *Angew. Chem., Int. Ed. Engl.* **2000**, *39*, 2268;

(16) In some experiments, the supercooled LC-phase of small portions of the material could even be observed at room temperature; however, their detailed investigation was not possible (see Supporting Information).

(17) Nonlinear regression analysis was used to fit the concentration C against the ^1H NMR chemical shifts δ, to iterate the chemical shifts at infinite dilution (δ_0) and complete association (δ_∞) to the theoretical equation (see, e.g.: Martin, R. B. *Chem. Rev.* **1996**, *96*, 3043):

$$\delta = \delta_0 + (\delta_\infty - \delta_0)\left(\frac{4KM_{tot} + 1 - \sqrt{8KM_{tot} + 1}}{4KM_{tot}}\right)$$

The addition of the nonsolvent hexane rapidly decreases the solubility of the compound. Therefore, the NMR signals could not be detected at higher concentrations, giving rise to an additional uncertainty of the dimerization constants.

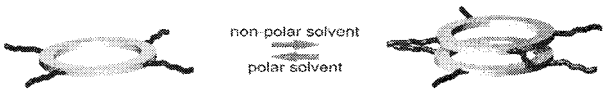

Figure 1. Schematic presentation of the solvent-induced macrocycle dimerization.

bically induced aggregation, Figure 1).[18,19] However, it must be pointed out that a further increase of the association constants by decreasing the volume fraction of the polar solvent is not possible due to the limited solubility of **1c** in hexane. Nevertheless, control of the degree of aggregation and ordering is indeed possible in this system that combines solvophobically induced aggregation with the formation of a soluble shell of the alkyl substituents.

This approach widely extends the possibility to form complex superstructures by the organization of cyclic moieties since it does not require a special electronic substitution pattern on the ring. Ongoing studies with rings containing noncrystallizable side groups will show if this approach can be extended toward the formation of hollow, cylinder-like molecular objects by a solvent-induced self-organization process.[3d,6,19]

Adsorption. A different approach toward the control of the organization of shape-persistent macrocycles is the formation of regular two-dimensional arrays. As Moore has shown, shape-persistent macrocycles with extraannular phenolic groups can form (quasi-) two-dimensional structures in the solid state. The driving force for this arrangement is the interaction of the polar groups of the macrocycles leading to an extended hydrogen-bonded network.[20]

However, the organization of nonfunctionalized rigid cyclic structures requires another driving force. One possible methodology should be the assembly of the objects at the air−water interface. Contrary to the expectations, Moore's phenylacetylene macrocycles studied on a Langmuir−Blodgett trough adopt at the interface an edge-on orientation, while the face-on orientation is not stable.[21]

Another approach toward regular 2D structures would be the adsorption of macrocycles from solution to the surface of highly oriented pyrolytic graphite (HOPG). In the case of our oligoalkyl substituted rings we expected that the lateral intermolecular interaction of the peripheric alkyl side chains and the balance between these groups and the hydrophobic HOPG substrate would drive the macrocycles to form well-ordered structures.[22] Ultimately, these 2D structures may provide a tool for epitaxially induced supramolecular 3D structures.[23]

Indeed, **1c** can be adsorbed at the solution−HOPG interface and forms a highly ordered and stable monolayer on the HOPG (001) surface. High-resolution scanning tunneling microscopy (STM) images show clearly two-dimensional structures of the macrocycles. The molecular image usually appeared immediately after bringing the solution of the ring in 1,2,4-trichlorobenzene onto the HOPG surface. During the first scan the image contrast of the **1c** adsorbates on HOPG varied spontaneously, yielding only fuzzy pictures. Then the observed structure was rather stable during repeated scanning by the STM tip at sufficiently low tunneling currents. Figure 2 shows a representative in situ STM image of a large scan area depicting boundaries between different domains. Within the domains superstructural arrays are seen aligned along particular directions. The angle between domain directions is 120° ± 3°, corresponding to the hexagonal graphite symmetry.[24]

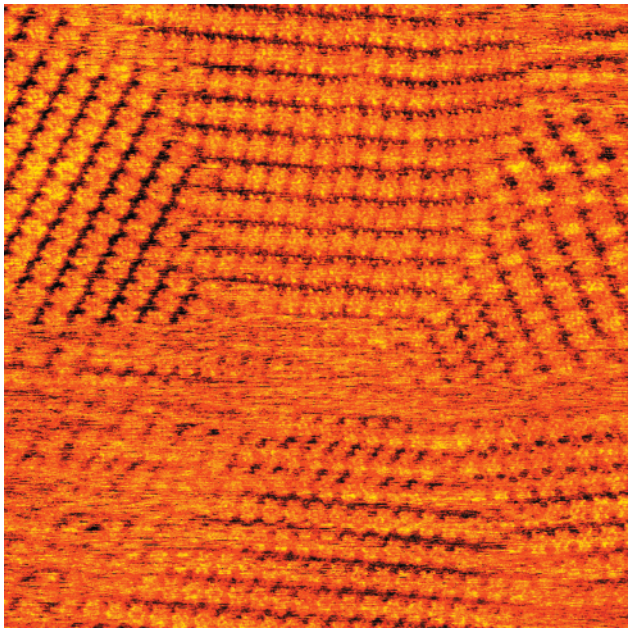

Figure 2. Monolayer domain structure of compound **1c** adsorbed from solution onto graphite. STM height image, size of 90 nm × 90 nm, height range 0.5 nm, $I = 8$ pA, $U = -500$ mV.

To study the arrangement of the molecules relative to the graphite lattice the underlying graphite was investigated by lowering the bias voltage (50 mV) at increased tunneling current (60 pA) (see inset in Figure 3). The high-resolution STM images reveal that the molecular rows were oriented with an angle of 31 ± 3° to the main crystallographic direction of the graphite. The peripheric alkyl tails of the macrocycles were oriented along the atomic rows of HOPG (001). The two-dimensional unit cell is of oblique symmetry (plane group $p1_2mm$), containing one macrocyclic molecule. The lattice constants were determined to be $A = 3.6 \pm 0.2$ nm, $B = 5.7 \pm 0.2$ nm, and $\Gamma = 74 \pm 3°$. Since the two-dimensional elementary cell is filled with only one molecue, the plane group implies C_2 symmetry for each molecule, including its alkyl periphery. These data suggest that the molecules cover the surface in the form of a densely packed monolayer with a tight arrangement of the alkyl chains that lie between the rows of the rings. A model of the molecular arrangement of the rings derived from the STM pictures is depicted in Figure 4. The size of individual macrocycle measured by STM is in agreement with the dimensions of the aromatic ring backbone determined by single-crystal X-ray analysis in similar compounds.[7a,15]

(18) For the solvophobic induced aggregation of branched noncovalent complexes see, e.g.: (a) Kraft, A.; Osterod, F.; Fröhlich, R. *J. Org. Chem.* **1999**, *64*, 6425. (b) Palmans, A. R. A.; Vekemans, J. A. J. M.; Havinge, E. E.; Meijer, E. W. *Angew. Chem.* **1997**, *109*, 2763; *Angew. Chem., Int. Ed. Engl.* **1997**, *36*, 2648.

(19) For reviews about low molecular mass organic gelators see, e.g.: (a) Terech, P.; Weiss, R. G. *Chem. Rev.* **1997**, *97*, 3133. (b) Abdallah, D. J.; Weiss, R. G. *Adv. Mater.* **2000**, *12*, 1237.

(20) Venkataraman, D.; Lee, S.; Zhang, J.; Moore, J. S. *Nature* **1994**, *371*, 591.

(21) Shetty, A. S.; Fischer, P. R.; Stork, K. F.; Bohn, P. W.; Moore, J. S. *J. Am. Chem. Soc.* **1996**, *118*, 9409.

(22) For 2D crystals of large polycyclic aromatic hydrocarbons on HOPG see, e.g.: Vivekanantan, S. I.; Yoshimura, K.; Enkelmann, V.; Epsch, R.; Rabe, J. P.; Müllen, K. *Angew. Chem.* **1998**, *110*, 2843; *Angew. Chem., Int. Ed. Engl.* **1998**, *37*, 2696;

(23) During the preparation of the manuscript the adsorption of cyclic thiophene oligomers on HOPG was independently reported by others: Krömer, J.; Rios-Carreras, I.; Fuhrmann, G.; Musch, C.; Wunderlin, M.; Debaerdemaeker, T.; Mena-Osteritz; E.; Bäuerle, P. *Angew. Chem.* **2000**, *112*, 3623; *Angew. Chem., Int. Ed. Engl.* **2000**, *39*, 3481.

(24) Spong, J. K.; Mizes, H. A.; LaComb, L. J., Jr.; Dovek, M. M.; Frommer, J. E.; Foster, J. S. *Nature* **1989**, *338*, 137.

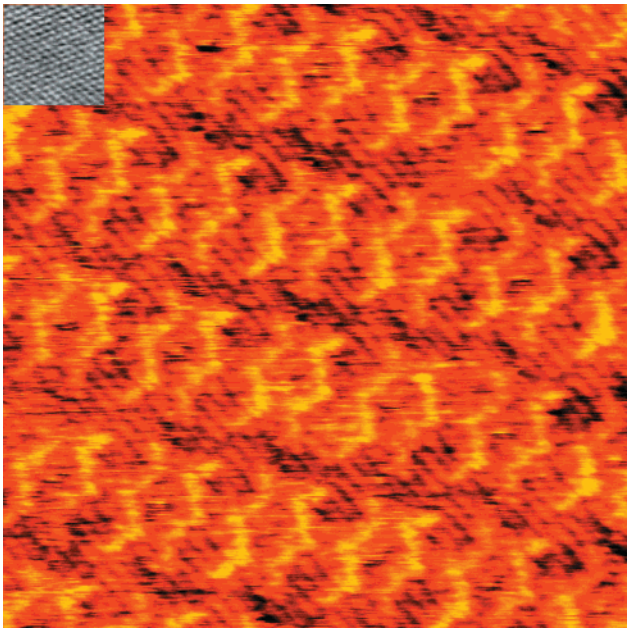

Figure 3. STM height image of the compound **1c** adsorbed on graphite. Image size 18.8 nm × 18.8 nm, the height range cover 0.5 nm, $I = 8$ pA, $U = -500$ mV. The inset shows an STM image of the underlying graphite lattice (side 3 nm, $I = 60$ pA, $U = -50$ mV).

Figure 5 displays two-high resolution images of the same region in which each aromatic system of the rings and the alkyl side chains are clearly visible. The most intriguing feature is that the unit cells of both micrographs show different contrast. In general, the image contrast depends on large variations of tunnel gap resistance ($R_{gap} = U/I$).[25] Our case is notable because only a 5% variation of R_{gap} affects the image contrast strongly. In both pictures the contrast variation between the aromatic ring and the alkyl side chains is clearly visible. Whereas in Figure 5A the cyclic backbone is represented with uniform intensity, in Figure 5B the diacetylene bridge cannot be seen. Hence, the contrast in the STM images relies strongly on the local electronic coupling of the adsorbed molecules with the surface and tip, and cannot be attributed simply to the topography.[26,27] To test this assumption, the frontier orbitals of the cyclic backbone of **1c** have been calculated by the MNDO method. The density of the lowest unoccupied molecular orbital (LUMO) is uniformly distributed over the whole ring (Figure 6A), while the density of the highest occupied molecular orbital (HOMO) exhibits distinct minima at the two diacetylene bridges (Figure 6B). Quantitatively, it can be inferred that the contrast is due to the perturbation of the frontier orbital by the presence of the tip−HOPG surface. Namely, the LUMO dominates the contrast in Figure 5A, while the HOMO contributes on the appearance of Figure 5B.

To understand the effect of the HOPG surface on the macrocycle, computer simulations of the cyclic backbone were performed with MacroModel 7.0[28] using the Merck molecular force field (MMFF).[29] The single cyclic macrocycle exhibits two energetically similar nonplanar molecular geometries, which are denoted the "boat" (Figure 7A) and the "chair" conformation (Figure 7B); the chair conformation is also found in the solid-state structure of similar rings.[7a,15] Figure 7D shows the potential curves obtained from the approximation of the macrocycles to the HOPG surface. At large distances ($d > 1.5$ nm, d is the shortest distance between the surface and a point defined as the intersection of lines between opposite located phenyl rings of the macrocycle) between substrate and adsorbate the flat conformation (Figure 7C) is less stable than the boat and the chair conformation by about 30 kJ/mol. However, this situation changes dramatically when the macrocycles were brought in contact with a graphite surface. Due to their nonplanar geometry the latter cannot approach the surface closely ($d > 0.6-0.8$ nm),

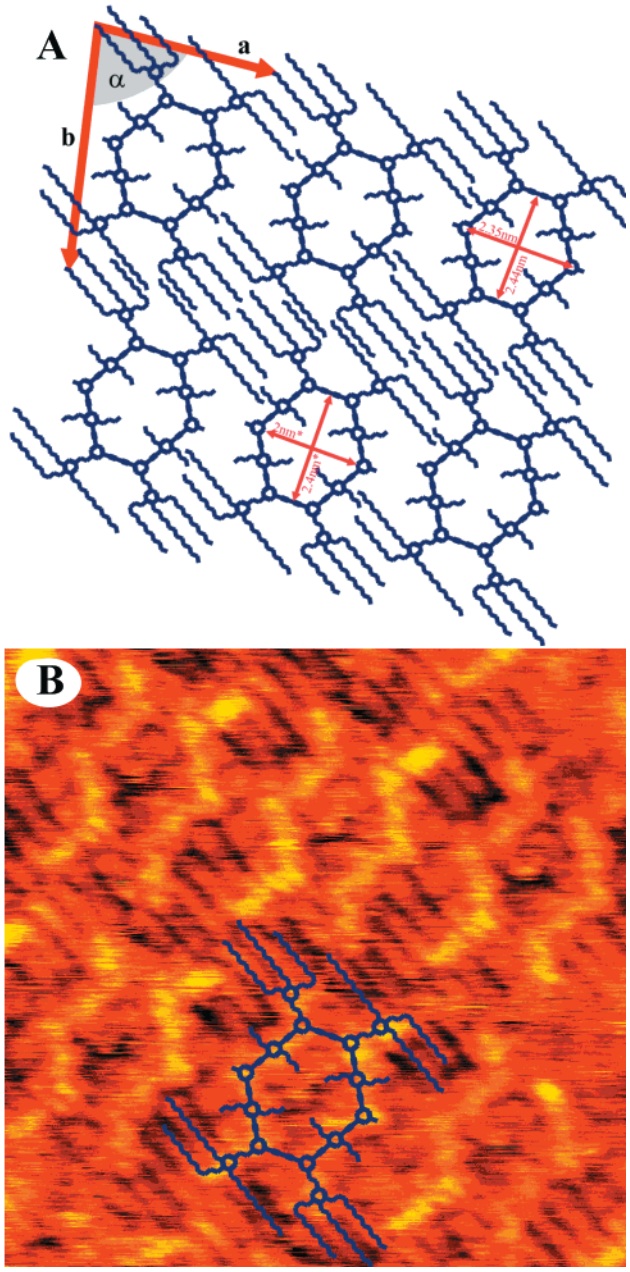

Figure 4. Possible structure of **1c** based on the registry of the alkyl side chains on the HOPG (001) surface (A and B). The dimensions of the aromatic backbone of an analogue compound obtained by single-crystal X-ray analysis are marked (*).

(25) At low magnification the interaction tip−sample, due to the scanning speed, affects the ordering of the adsorbed molecules. The true structure of the monolayer is deduced from the high magnification micrographs showing. Careful examination shows the presence of local hexagonal symmetry in all cases.

(26) Foster, J. S.; Frommer, J. E. *Nature* **1988**, *333*, 542.

(27) (a) Lazzaroni, R.; Calderone, A.; Lambin, G.; Rabe, J. P.; Brédas, J. L. *Synth. Met.* **1991**, *525*, 41. (b) Lazzaroni, R.; Calderone, A.; Brédas, J. L.; Rabe, J. P. *J. Phys. Chem.* **1997**, *107*, 99.

(28) Mohamadi, F.; Richards, N. G. J.; Guida, W. C.; Liskamp, R.; Lipton, M.; Caulfield, C.; Chang, G.; Hendrickson, T.; Still, W. C. *J. Comput. Chem.* **1990**, *11*, 440.

(29) Halgren, T. A. *J. Comput. Chem.* **1996**, *17*, 490.

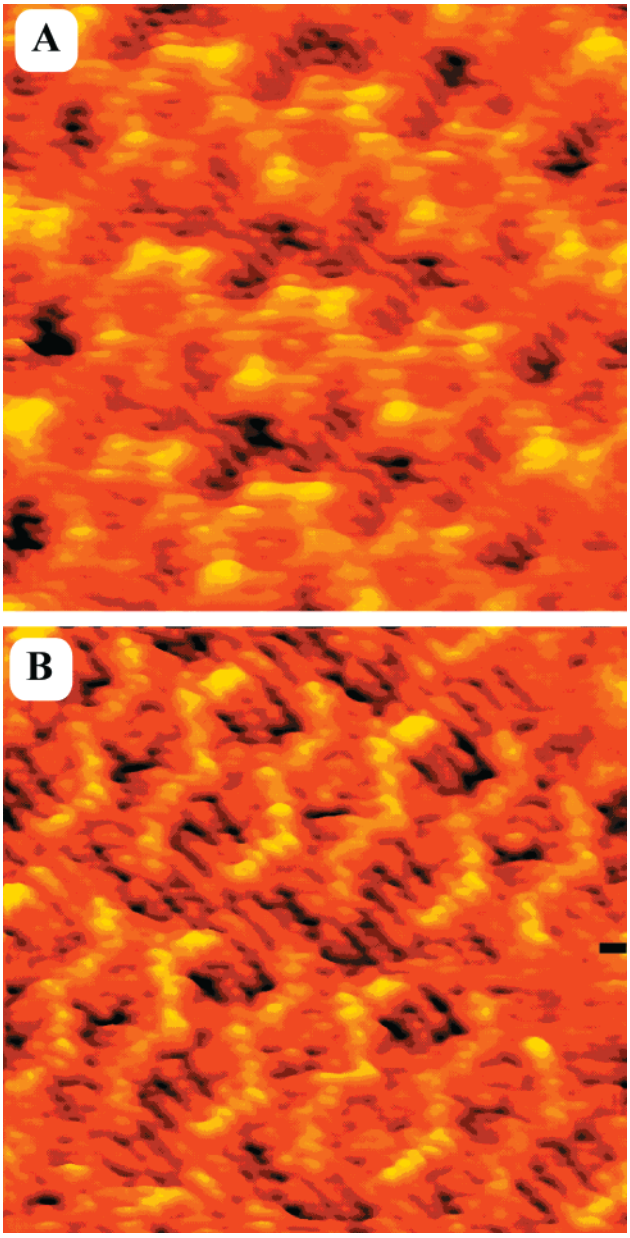

Figure 5. STM height images of **1c** on the HOPG (001) surface. Scan area: 10.4 nm × 10.4 nm. (A) $I = 8.79$ pA and $U = -1$ V, (B) $I = 9.24$ pA and $U = -1$ V.

while the flat conformation can reach a minimum distance of 0.4 nm. The calculated difference in adsorption enthalpy is larger than the difference of the three conformations. Hence, the potential curves predict the transition from the nonplanar to the flat conformation during the adsorption process. The driving force for this change in molecular conformation is the optimization of the contact area between the aromatic units and the graphite surface, since the aliphatic units were not considered in the calculation (see Supporting Information).[30]

Our STM investigation clearly demonstrates that the macrocycle **1c** adsorbs on HOPG surface in a two-dimensional ordered monolayer. The strong interaction between the substrate and the adsorbates caused a sufficient flattening of the shape-persistent macrocycle. The assembly of macrocycles onto the graphite surface could be a valuable tool for surface patterning in the nanometer regime. Patterning could be achieved by a judicious choice of macrocycle size and specific functionality, allowing one to pattern the surface with a "bottom-up" approach.

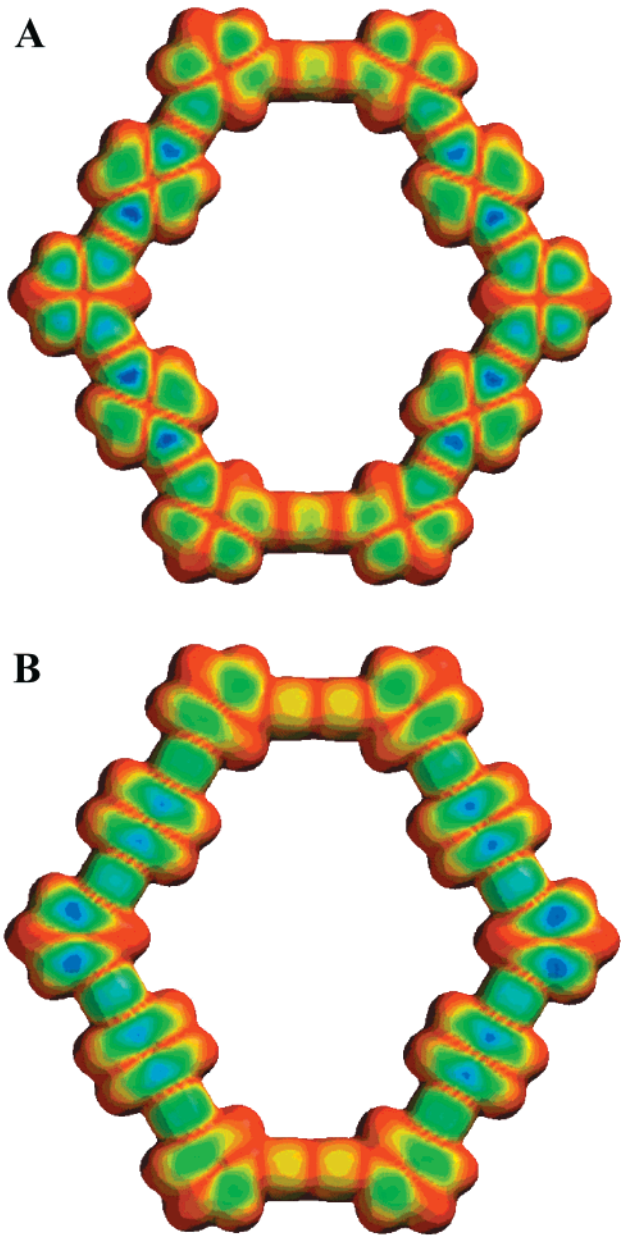

Figure 6. (A) LUMO, and (B) HOMO of the cyclic backbone of **1c**. Result of the MNDO calculation using SPARTAN1.3.5.

The use of functionalized macrocycles for the preparation of functionalized nano-patterned surfaces is in progress.

Conclusions

We have described the synthesis of shape-persistent macrocycles with four phenol OH groups pointing to the outside, allowing the attachment of alkyl- and branched oligoalkyl-substituents to the rings. In solution, the aggregation of the macrocycles can be influenced by changing the solvent properties. In good solvents for both the stiff core and the flexible extraannular alkyl chains (CD_2Cl_2), no aggregation was observed. However, by adding a nonsolvent with respect to the core (*n*-hexane-d_{14}), the rings tend to aggregate. The degree of association increases as the polarity of the solvent mixture decreases.

(30) Linear paraffins are known to absorb strongly on HOPG. Hence, the interaction between **1c** and HOPG is underestimated by our calculations, e.g.; Rabe, J. P.; Buchholz, S. *Phys. Rev. Lett.* **1991**, *66*, 2096.

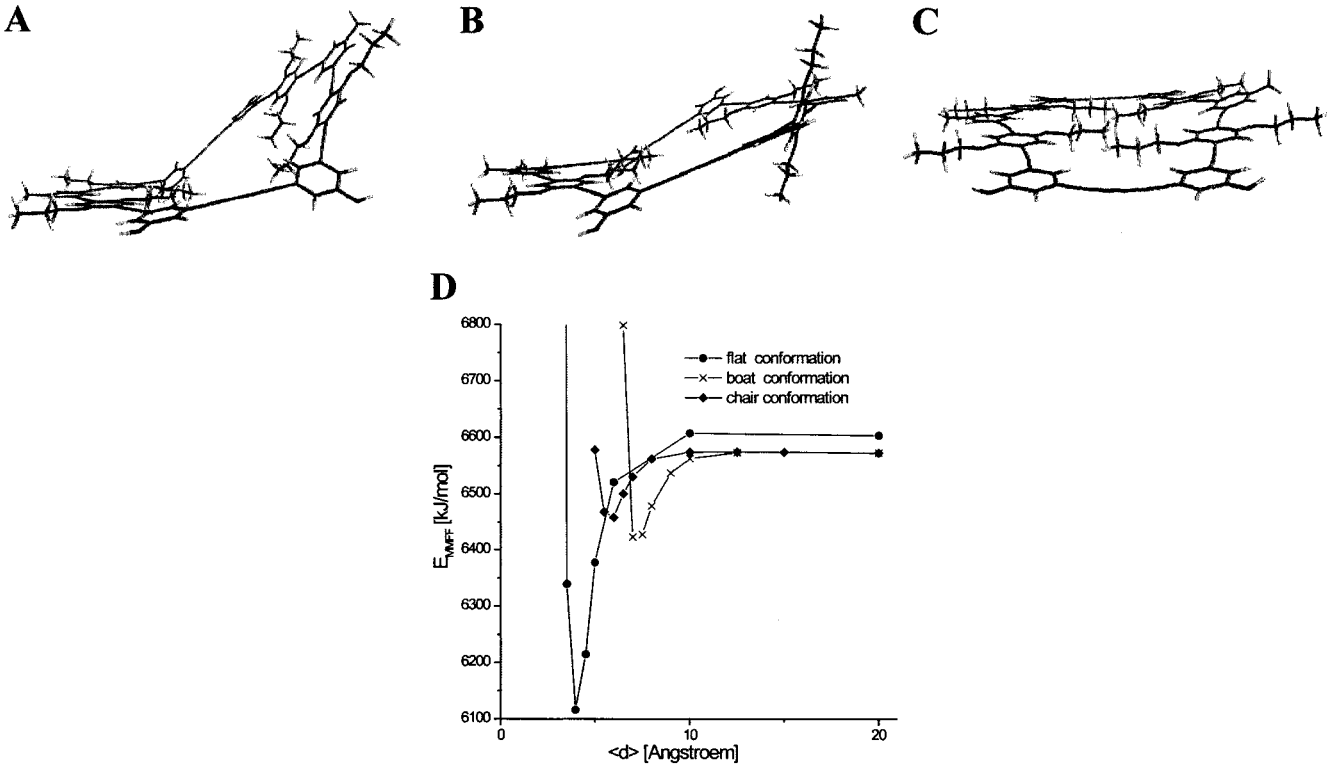

Figure 7. Boat (A), chair (B), and planar (C) conformation of the macrocycle and potential curves of their approximation to the HOPG surface (D).

Apart from the possibility to organize the macrocycles by aggregation, it is possible to use the adsorption on HOPG to obtain a two-dimensional arrangement of the rings. Our previous work on the synthesis of functionalized macrocycles should enable us to pattern the surface on a nanoscale with various functionalities, and subsequently use these structures as a platform for the formation of 3D supramolecular structures.

Experimental Section

General Methods. Commercially available chemicals were used as received. THF was distilled from potassium prior to use. Piperidine and pyridine were distilled from CaH_2 and stored under argon. ^{1}H NMR and ^{13}C NMR spectra were recorded on Bruker AC-300 (300 MHz for proton 75.48 MHz for carbon). Thin-layer chromatography was performed on aluminum plates precoated with Merck 5735 silica gel 60 F_{254}. Column chromatography was performed with Merck silica gel 60 (230−400 mesh). Radial chromatography was performed with Merck silica gel 60 PF_{254} containing $CaSO_4$. The gel permeation chromatograms were measured in THF (flow rate 1 mL min^{-1}) at room temperature, using a combination of three styragel columns (porosity 10^3, 10^5, and 10^6) and an UV detector operating at $\lambda = 254$ nm. The molecular weight was obtained from polystyrene calibrated SEC columns. The matrix-assisted laser desorption ionization time-of-flight measurements were carried out on a Bruker reflex spectrometer (Bruker, Bremen), incorporating a 337 nm nitrogen laser with a 3 ns pulse duration (10^6−10^7 W cm^{-1}, 100 μm spot diameter). The instrument was operated in a linear mode with an accelerating potential of 33.65 kV. The mass scale was calibrated using polystyrene ($M_p = 4700$), using a number of resolved oligomers. Samples were prepared by dissolving the macrocycle in THF at a concentration of 10^{-4} mol L^{-1}. Then 10 μL of this solution and 10 μL of a 10^{-3} mol l^{-1} silver trifluoroacetate solution were added to 10 μL of a 0.1 mol L^{-1} matrix solution, dissolved in THF. In all cases 1,8,9-trihydroxyanthracene (Aldrich, Steinheim) was used as matrix. Then1 μL of this mixture was applied to the multistage target and airdried. Microanalysis was performed by the University of Mainz. Scanning tunneling microscopy (STM) measurements were carried out at ambient conditions with a low-current RHK 1000 control system. In situ STM imaging was performed at the internal interface between HOPG and concentrated solution of **1c** dissolved in 1,2,4-trichlorobenzene. A drop of solution was placed on a freshly cleaved HOPG surface, while the surface had already been scanned by STM under conditions that allowed atomic resolution of the graphite surface structure. A potential of $V = \pm 1$ V was applied to the substrate. The scan rate was varied between 0.2 and 0.6 μm/s. The tunneling current set point was 8−20 pA. All images presented were obtained at constant current mode using a Pt/Ir (90/10)-tip, which was mechanically sharpened. The specific tunneling conditions are given in the figure captions. Molecular Modeling was performed with MacroModel 7.0,[28] using the Merck molecular force field (MMFF).[29] Structure optimization was performed by application of the Polak-Ribier algorithm[31] to random start conformations until a final gradient below 0.005 kJ/Å was reached. The structure was refined further by means of the Truncated Newton conjugate gradient methode[32] until the final gradient was below 0.005 kJ/Å. A HOPG surface was simulated by two layers of polycyclic aromates of sufficient lateral extension to cover the adsorbed species. Semiempirical calculations were done with SPARTAN 5.1.3, using the MNDO option. The default convergence criterion was used (rms change in density matrix <0.001, self-consistent field energy convergence: $<10^{-6}$ eV. No symmetry condition was applied. Convergence criterion was met after 3494 cycles).

1,4-Dipropyloxy-2-(2-triisopropylsilylethynyl)-5-(2-trimethylsilylethinyl)benzene (3). $Pd(PPh_3)_2Cl_2$ (300 mg) and CuI (150 mg) were added to a solution of 4-bromo-2,5-dipropyloxy-iodobenzene (12.0 g, 30.0 mmol), triisopropylsilylacetylene (5.85 g, 32.0 mmol), and PPh_3 (300 mg) in piperidine (60 mL) at 0 °C. The mixture was allowed to reach room temperature and was stirred for 2 days, followed by an additional 2 days at 55 °C. Then trimethylsilylacetylene (5.89 g, 60.0 mmol) was added, and the mixture was stirred for an additional 2 days at the same temperature. After the reaction mixture cooled to room temperature, ether and water were added. The organic phase was separated and extracted with water, 10% acetic acid, water, 10%

(31) Polak, E.; Ribiere, G. *Rev. Franc. Informat. Rech. Operat.* **1969**, *35*, 16.

(32) Ponder, J. W.; Richardson, F. M. *J. Comput. Chem.* **1987**, *8*, 1016.

aqueous sodium hydroxide, water, and brine, and then dried over $MgSO_4$. Evaporation of the solvent yielded a brown residue that was filtered over silica gel with petroleum ether/ether (10:1) as the eluent ($R_f = 0.90$) and recrystallized from methanol to give **4** as a colorless powder (11.9 g, 84%) mp 89 °C; ^{1}H NMR (CD_2Cl_2) δ 6.92 (s, 1 H), 6.90 (s, 1 H), 3.93 (t, $J = 6.5$ Hz, 2 H), 3.91 (t, $J = 6.5$ Hz, 2 H), 1.80 (m, 4 H), 1.15 (s, 21 H), 1.07 (t, $J = 7.4$ Hz, 3 H), 0.26 (s, 9 H);^{13}C NMR (CD_2Cl_2) δ 154.61, 154.07, 117.92, 116.90, 114.43, 114.11, 103.08, 101.31, 99.98, 96.70, 71.36, 71.06, 22.89, 22.82, 18.60, 11.57, 10.48, 10.41, −0.27. MS (EI) $m/z = 470.2$ (75) [M^+], 427.1 (29), 385.2 (25), 343.1 (22), 315.1 (15), 298.9 (15), 270.9 (17), 73.0 (100). Anal. Calcd for $C_{30}H_{46}O_2Si_2$ (470.84): C, 71.43; H, 9.85. Found: C, 71.06; H, 9.81.

1,4-Dipropyloxy-2-ethynyl-5-(2-triisopropylsilylethynyl)benzene (4). Compound **3** (4.71 g, 10.0 mmol) was dissolved in MeOH/THF (1:1, 30 mL), K_2CO_3 (4.1 g, 30 mmol) was added, and the mixture was stirred overnight. The mixture was poured into ether and water, and the organic layer was extracted with water and brine. Drying over $MgSO_4$ and subsequent evaporation of the solvent yielded a yellow residue that was purified by column chromatography over silica gel with hexanes/CH_2Cl_2 (7:1) as the eluent ($R_f = 0.34$) to give **5** as a slightly yellow solid (3.75 g, 94%) mp 97 °C; ^{1}H NMR (300 MHz, CD_2Cl_2) δ 6.94 (s, 2 H), 3.94 (t, $J = 6.5$ Hz, 2 H), 3.91 (t, $J = 6.5$ Hz, 2 H), 3.37 (s, 1 H), 1.81 (m, 4 H), 1.15 (m, 21 H), 1.07 (t, $J = 6.5$ Hz, 3 H), 1.05 (t, $J = 6.5$ Hz, 3 H); ^{13}C NMR (75.45 MHz, CD_2Cl_2) δ 154.31, 154.16, 117.68, 117.59, 114.85, 112.88, 102.95, 96.83, 82.25, 80.12, 71.33, 71.15, 22.85, 22.82, 18.64, 11.76, 10.73, 10.40; MS (FD) m/z 398.1 [M^+]. Anal. Calcd for $C_{25}H_{38}O_2Si$ (398.66): C, 75.32; H 9.61. Found C, 75.32; H, 9.68.

3,5-Bis-{2-[2,5-dipropyloxy-4-(2-triisopropylsilylethynyl)phenyl]-ethynyl}toluene (6). $Pd(PPh_3)_2Cl_2$ (150 mg) and CuI (80 mg) were added to a solution of **4** (8.02 g, 20.1 mmol), 3,5-diiodotoluene (3.27 g, 9.50 mmol), and PPh_3 (150 mg) in piperidine (100 mL). The solution was stirred for 24 h at room temperature and then poured into ether and water. The organic phase was separated and extracted with water, 10% acetic acid, water, 10% aqueous sodium hydroxide, water, and brine. Drying over $MgSO_4$ and evaporation of the solvent yielded an oily residue that was chromatographed over silica gel with CH_2Cl_2/hexanes (1:3) as the eluent ($R_f = 0.42$) to give **6** as a slightly yellow solid (7.2 g, 86%). ^{1}H NMR (300 MHz, CD_2Cl_2) δ 7.47 (s, 1 H), 7.32 (br s, 2 H), 6.98 (s, 2 H), 6.96 (s, 2 H), 3.98 (t, $J = 6.5$ Hz, 4 H), 3.94 (t, $J = 6.5$ Hz, 4 H), 2.36 (s, 3 H), 1.83 (m, 8 H), 1.15 (m, 42 H), 1.10 (t, $J = 7.4$ Hz, 3 H), 1.05 (t, $J = 7.4$ Hz, 3 H); ^{13}C NMR (75.45 MHz, CD_2Cl_2) δ 154.93, 154.13, 139.29, 132.68, 131.87, 124.25, 118.29, 117.27, 114.88, 114.47, 103.61, 97.27, 94.47, 86.87, 71.89, 71.61, 23.40, 23.33, 21.43, 12.03, 10.99, 10.95; MS (FD) m/z 885.3 [M^+].

3,5-Bis-[2-(2,5-dipropyloxy-4-ethynylphenyl)-ethynyl]toluene (7). A 1 M solution of Bu_4NF in THF (13.5 mL, 13.5 mmol) was added to a solution of **6** (3.00 g, 3.39 mmol) in THF (20 mL). The mixture was stirred for 2 h at room temperature and then poured into ether and water. The organic layer was extracted with water and brine and dried over $MgSO_4$. Evaporation of the solvent yielded a slightly yellow-brown oil, which was purified by chromatography over silica gel with hexanes/CH_2Cl_2 (1:1) as the eluent ($R_f = 0.72$) to give **7** as a slightly yellow solid (1.82 g, 94%) mp 112 °C; ^{1}H NMR (300 MHz, CD_2Cl_2) δ 7.49 (m, 1 H), 7.34 (m, 2 H), 7.02 (s, 2 H), 7.00 (s, 2 H), 3.98 (t, $J = 6.5$ Hz, 4 H), 3.97 (t, $J = 6.5$ Hz, 4 H), 3.40 (s, 2 H), 2.37 (s, 3 H), 1.84 (m, 8 H), 1.10 (t, $J = 7.4$ Hz, 6 H), 1.06 (t, $J = 7.4$ Hz, 6 H); ^{13}C NMR (75.45 MHz, CD_2Cl_2) δ 154.28, 153.64, 138.82, 132.26, 131.42, 123.66, 118.02, 117.09, 114.50, 112.91, 94.08, 86.09, 82.36, 80.01, 71.30, 71.20, 22.82, 22.72, 20.92, 10.41, 10.31; MS (FD) m/z 572.2 [M^+] Anal. Calcd for $C_{39}H_{40}O_4$ (572.74): C, 81.79; H, 7.04. Found: C, 81.76; H, 7.08.

3,5-Diiodo-(tetrahydro-*2H*-pyran-2-yloxy)benzene (8). *p*-Toluenesulfonic acid (∼30 mg) was added to a solution of 3,5-diiodophenol (11.3 g, 32.7 mmol) and of 3,4-dihydro-(2H)-pyran (13.5 g, 160 mmol) in CH_2Cl_2 (100 mL) at 0 °C. The solution was stirred for 2 h at this temperature and subseqently for 45 min at room temperature before being poured into ether and 10% aqueous sodium hydroxide. The organic phase was separated and washed with 10% aqueous sodium hydroxide, water, and brine and then dried over $MgSO_4$. Evaporation of the solvent yielded a slightly yellow oil, which was chromatographed over silica gel with hexanes/CH_2Cl_2 (2:1) as the eluent ($R_f = 0.77$). The solvent was removed to give **8** as colorless solid (12.1 g, 86%) mp 57−59 °C; ^{1}H NMR (300 MHz, CD_2Cl_2) δ 7.68 (m, 1 H), 7.39 (m, 2 H), 5.37 (t, $J = 3.0$ Hz, 1 H), 3.79 (m, 1 H), 3.59 (m, 1 H), 2.00−1.60 (m, 6 H); ^{13}C NMR (75.45 MHz, CD_2Cl_2) δ 158.05, 138.37, 125.45, 96.81, 94.26, 62.09, 30.16, 25.13, 18.49; MS (FD) m/z 430.0 [M^+] Anal. Calcd for $C_{11}H_{12}O_2I_2$ (430.02): C, 30.72; H, 2.81. Found: C, 30.69; H, 2.75.

3,5-Bis-[2-(2,5-dipropyloxy-4-{2-[5-iod-3-(tetrahydro-*2H*-pyran-2-yloxy)phenyl]ethynyl}phenyl)ethynyl]toluene (9). $Pd(PPh_3)_2Cl_2$ (40 mg) and CuI (20 mg) were added to a solution of **8** (9.50 g, 22.1 mmol), **7** (2.10 g, 3.68 mmol), and PPh_3 (40 mg) in piperidine (20 mL), and the mixture was stirred for 12 h at 60 °C. Workup was performed as described for compund **6**. The oily crude product was chromatographed over silica gel with CH_2Cl_2/hexanes (1:2) as the eluent to recover most of the excess of **8** ($R_f = 0.77$). Changing the eluent to CH_2Cl_2/hexanes (1:1) yielded as second fraction ($R_f = 0.50$) **9** as a slightly yellow solid (2.77 g, 64%). ^{1}H NMR (300 MHz, CD_2Cl_2) δ 7.51 (t, $J = 1.5$ Hz, 2 H), 7.50 (m, 1 H), 7.41 (dd, $^1J = 1.3$ Hz, $^2J = 1.5$ Hz, 2 H), 7.34 (m, 2 H), 7.19 (dd, $^1J = 1.2$ Hz, $^2J = 2.3$ Hz, 2 H), 7.04 (s, 2 H), 7.03 (s, 2 H), 5.41 (t, $J = 3.1$ Hz, 2 H), 4.00 (t, $J = 6.4$ Hz, 8 H), 3.84 (m, 2 H), 3.63 (m, 2 H), 2.37 (s, 3 H), 2.00−1.60 (m, 20 H), 1.11 (t, $J = 7.2$ Hz, 6 H), 1.10 (t, $J = 7.2$ Hz, 6 H); ^{13}C NMR (75.45 MHz, CD_2Cl_2) δ 157.52, 153.88, 153.82, 138.83, 133.44, 132.25, 131.42, 126.30, 126.00, 123.71, 118.93, 117.21, 117.25, 114.33, 113.74, 96.87, 94.24, 93.52, 92.95, 87.11, 86.28, 71.32, 62.19, 30.29, 25.22, 22.83, 20.92, 18.68, 10.43; MS (FD) m/z 1176.3 [M^+]. Anal. Calcd for $C_{61}H_{62}I_2O_8$ (1176.96): C, 62.25; H, 5.31. Found: C, 62.48; H, 5.32.

3,5-Bis-[2-(2,5-dipropyloxy-4-{2-[3-(tetrahydro-*2H*-pyran-2-yloxy)-5-(2-trimethylsilylethynyl)phenyl]ethynyl}phenyl)ethynyl]toluene (10). $Pd(PPh_3)_2Cl_2$ (20 mg) and CuI (10 mg) were added to a solution of **9** (1.05 g, 0.93 mmol), TMS acetylene (0.55 g, 5.6 mmol), and PPh_3 (20 mg) in piperidine (20 mL), and the mixture was stirred for 12 h at 60 °C. Workup was performed as described for compund **6**. Column chromatography over silica gel with CH_2Cl_2/hexanes (1:1) as the eluent ($R_f = 0.54$) gave **10** as a slightly yellow oil which slowly solidified (0.95 g, 91%). ^{1}H NMR (300 MHz, CD_2Cl_2) δ 7.50 (m, 1 H), 7.34 (m, 2 H), 7.24 (m, 2 H), 7.18 (dd, $^1J = 1.5$ Hz, $^2J = 2.3$ Hz, 2 H), 7.12 (m, 2 H), 7.04 (s, 3 H), 7.03 (s, 3 H), 5.43 (m, 2 H), 4.01 (t, $J = 6.5$ Hz, 8 H), 3.86 (m, 2 H), 3.63 (m, 2 H), 2.38 (s, 3 H), 2.00−1.60 (m, 20 H), 1.12 (t, $J = 7.5$ Hz, 6 H), 1.11 (t, $J = 7.5$ Hz, 6 H), 0.26 (s, 18 H); ^{13}C NMR (75.45 MHz, CD_2Cl_2) δ 157.02, 153.83, 138.83, 132.23, 131.41, 128.26, 124.64, 124.50, 123.73, 120.08, 120.00, 117.25, 114.17, 113.96, 104.01, 96.73, 94.88, 94.16, 93.85, 86.43, 86.30, 71.32, 62.17, 30.34, 29.26, 22.84, 20.93, 18.75, 10.42, −0.36; MS (FD) m/z 1117.0 [M^+].

3,5-Bis-[2-(2,5-dipropyloxy-4-{2-[3-(tetrahydro-*2H*-pyran-2-yloxy)-5-ethynylphenyl]ethynyl}phenyl)ethynyl]toluene (11). Compound **11** was prepared by the procedure described for **4**, with **10** (1.50 g, 1.34 mmol), K_2CO_3 (0.93 g, 6.7 mmol) and MeOH/THF (1:1, 40 mL). Purification was performed by column chromatography (silica gel) with hexanes/ethyl acetate (3:1) as the eluent ($R_f = 0.62$) to give **11** in nearly quantitative yield as a slightly yellow oil that slowly solidified. ^{1}H NMR (300 MHz, CD_2Cl_2) δ 7.50 (br s, 1 H), 7.35 (br s, 2 H), 7.28 (m, 2 H), 7.22 (m, 2 H), 7.16 (m, 2 H), 7.04 (m, 4 H), 5.42 (m, 2 H), 4.01 (t, $J = 6.1$ Hz, 8 H), 3.86 (m, 2 H), 3.61 (m, 2 H), 3.15 (s, 2 H), 2.38 (s, 3 H), 1.50−2.00 (m, 20 H), 1.12 (t, $J = 7.2$ Hz, 3 H), 1.11 (t, $J = 7.2$ Hz, 3 H); ^{13}C NMR (75.45 MHz, CD_2Cl_2) δ 157.08, 153.89, 153.83, 138.83, 132.23, 131.42, 128.39, 124.77, 123.72, 123.42, 120.50, 120.25, 117.27, 114.24, 113.89, 96.84, 94.19, 93.71, 86.54, 86.29, 82.68, 77.53, 71.33, 62.23, 30.35, 25.25, 22.84, 20.92, 18.79, 10.43; MS (FD) m/z 972.7 [M^+]. Anal. Calcd for $C_{65}H_{60}O_8$ (973.21): C, 80.22; H, 6.63. Found: C, 80.30; H, 6.91.

THP-Protected Macrocycle 12. A solution of **11** (1.8 g, 1.85 mmol) in pyridine (35 mL) was added to a suspension of CuCl (10.2 g, 103 mmol) and $CuCl_2$ (2.0 g, 15 mmol) in pyridine (250 mL) over 96 h at 60 °C. After the completion of the addition, the mixture was allowed to stir for an additional 4 d at room temperature and then was poured into CH_2Cl_2 and water. The organic phase was extracted with water, 25% NH_3 solution (in order to remove the copper salts), water, 10%

acetic acid, water, 10% aqueous sodium hydroxide, and brine and dried over $MgSO_4$. After evaporation of the solvent to about 30 to 40 mL, the coupling products were precipitated by the addition of methanol (200 mL) and collected by filtration. Recrystallization from pyridine gave **12** as a slightly yellow solid (0.86 g; 48%) mp 240 °C dec; ^{1}H NMR (300 MHz, CD_2Cl_2) δ 7.49 (m, 2 H), 7.34 (m, 4 H), 7.32 (m, 4 H), 7.25 (m, 4 H), 7.22 (m, 4 H), 7.12 (s, 4 H), 7.11 (s, 4 H), 5.52 (m, 4 H), 4.04 (t, J = 6.2 Hz, 16 H), 3.83 (m, 4 H), 3.62 (m, 4 H), 2.37 (s, 6 H), 2.00−1.50 (m, 40 H), 1.14 (t, J = 7.5 Hz, 24 H); ^{13}C NMR (75.45 MHz, d_8-THF) δ 158.29, 154.89, 154.79, 139.46, 132.85, 132.37, 129.71, 126.18, 124.94, 123.64, 121.28, 120.80, 117.88, 115.28, 114.74, 97.40, 94.70, 94.06, 87.82, 87.28, 81.57, 74.49, 71.77, 62.37, 31.03, 26.10, 23.63, 21.05, 19.40, 10.93; MS (MALDI-TOF) m/z 2052.4 [M + Ag]$^+$.

Macrocycle 13. To a suspension of **12** (500 mg, 0.26 mmol) in $CHCl_3$ (200 mL) was slowly added MeOH (15 mL) and then *p*-toluenesulfonic acid (10−15 mg). The mixture was stirred for 3 d at room temperature under an argon atmosphere. Methanol was added, and the yellow precipitate was collected by filtration and vacuum-dried in the dark to give **13** as a slightly yellow solid (436 mg; 98%) mp 240 °C dec; ^{1}H NMR (300 MHz, d_7-DMF, 80 °C) δ = 10.10 (br s, 4 H), 7.55 (s, 2 H), 7.43 (m, 4 H), 7.28 (m, 12 H), 7.13 (m, 8 H), 4.15 (t, J = 6.3 Hz, 8 H), 4.14 (t, J = 6.3 Hz, 8 H), 2.43 (s, 6 H), 1.95−1.80 (m, 16 H), 1.15 (m, 24 H); ^{13}C NMR (75.45 MHz, d_7-DMF, 80 °C) δ 159.51, 155.23, 140.45, 132.90, 132.60, 127.90, 126.25, 124.98, 123.74, 120.80, 120.30, 119.06, 119.01, 115.57, 115.38, 95.10, 94.77, 87.91, 87.83, 82.36, 74.60, 72.58, 23.73, 21.34, 11.13; MS (MALDI-TOF) m/z 1712.9 [M + Ag]$^+$.

Macrocycle 1a. K_2CO_3 (520 mg, 3.7 mmol) was added to a solution of **13** (150 mg, 94 μmol) and stearylbromide (138 mg, 0.42 mmol) in DMF (60 mL) at 60 °C and stirred for 4 d at the same temperature in the dark. After the reaction mixture cooled to room temperature, CH_2Cl_2 and water were added. The organic phase was separated and extracted with water and brine and dried over $MgSO_4$. After evaporation of the solvent the residue was chromatographed over silica gel with hexanes/CH_2Cl_2 (1:3) as the eluent (R_f = 0.57) to give **1a** as a slightly yellow powder (34 mg, 14%): mp 220−222 °C; ^{1}H NMR (300 MHz, CD_2Cl_2) δ 7.54 (m, 2 H), 7.33 (m, 4 H), 7.32 (m, 4 H), 7.09 (m, 4 H), 7.06 (m, 8 H), 7.04 (m, 4 H), 4.08−3.98 (m, 24 H), 2.39 (s, 6 H), 2.00−1.75 (m, 24 H), 1.45−1.25 (m, 120 H), 1.14 (t, J = 7.6 Hz, 24 H), 0.90 (m, 12 H); ^{13}C NMR (75.45 MHz, CD_2Cl_2) δ 159.30, 154.06, 153.98, 138.91, 132.02, 128.40, 125.17, 123.83, 123.00, 118.83, 118.39, 117.48, 117.42, 114.53, 113.97, 94.30, 93.66, 86.86, 86.36, 81.09, 73.93, 71.50, 68.79, 41.36, 32.09, 29.85, 29.81, 29.75, 29.72, 29.50, 29.27, 26.11, 22.93, 22.83, 13.97, 10.47; MS (FD) m/z 2614.5 [M$^+$]; $C_{182}H_{236}O_{12}$ (2615.81).

Macrocycle 1b. Compound **1b** was prepared by the procedure described for **1a**, by adding K_2CO_3 (690 mg, 5.0 mmol) to a solution of **13** (200 mg, 125 μmol) and 3,4,5-trihexyloxy benzyl chloride (234 mg, 0.55 mmol) in DMF (130 mL). Purification was performed by repeated column chromatography over silica gel with hexanes/CH_2Cl_2 (2:3) as the eluent (R_f = 0.24) to give **1b** as a slightly yellow powder (190 mg, 48%) mp 202−204 °C; ^{1}H NMR (300 MHz, CD_2Cl_2) δ 7.53 (m, 2 H), 7.36 (t, J = 1.4 Hz, 4 H), 7.34 (dd, ^1J = 1.4 Hz, ^2J = 0.8 Hz, 4 H), 7.17 (dd, ^1J = 2.5 Hz, ^2J = 1.4 Hz, 4 H), 7.11 (dd, ^1J = 2.5 Hz, ^2J = 1.4 Hz, 4 H), 7.05 (m, 8 H), 6.63 (m, 8 H), 4.05−3.90 (m, 40 H), 2.38 (s, 6 H), 1.95−1.65 (m, 40 H), 1.55−1.25 (m, 72 H), 1.13 (t, J = 7.4 Hz, 12 H), 1.12 (t, J = 7.4 Hz, 12 H), 0.91 (m, 36 H); ^{13}C NMR (75.45 MHz, CD_2Cl_2) δ 158.82, 153.96, 153.85, 153.50, 138.89, 138.18, 131.93, 131.34, 128.83, 125.22, 123.72, 123.00, 119.09, 118.53, 117.27, 114.45, 113.71, 106.16, 94.28, 93.44, 87.03, 86.28, 80.97, 74.02, 73.48, 71.35, 70.86, 69.27, 31.90, 31.73, 30.43, 29.53, 25.90, 22.87, 22.81, 22.75, 20.96, 13.95, 13.90, 10.45; MS (MALDI-TOF) m/z 3275.48 [M + Ag$^+$]; $C_{210}H_{260}O_{24}$ (3168.30).

Macrocycle 1c. Compound **1c** was prepared by the procedure described for **1a**, by adding K_2CO_3 (690 mg, 5.0 mmol) to a solution of **13** (200 mg, 125 μmol) and 3,4,5-tridodecyloxy benzyl chloride (373 mg, 0.55 mmol) in DMF (130 mL). Purification was performed by repeated column chromatography over silica gel with hexanes/CH_2Cl_2 (1:1) as the eluent (R_f = 0.36) to give **1a** as a slightly yellow solid (167 mg, 32%) mp 122−126 °C; ^{1}H NMR (300 MHz, CD_2Cl_2) δ 7.52 (m, 2 H), 7.36 (t, J = 1.4 Hz, 4 H), 7.34 (dd, ^1J = 1.4 Hz, ^2J = 0.8 Hz, 4 H), 7.17 (dd, ^1J = 2.5 Hz, ^2J = 1.4 Hz, 4 H), 7.11 (dd, ^1J = 2.2 Hz, ^2J = 1.4 Hz, 4 H), 7.05 (m, 8 H), 6.63 (s, 8 H), 4.98 (s, 8 H), 4.05−3.90 (m, 40 H), 2.38 (s, 6 H), 1.95−1.65 (m, 40 H), 1.50−1.20 (m, 216 H), 1.12 (t, J = 7.4 Hz, 12 H), 1.13 (t, J = 7.4 Hz, 12 H), 0.88 (m, 36 H); ^{13}C NMR (125 MHz, CD_2Cl_2) δ 158.79, 153.94, 153.82, 153.47, 138.87, 138.13, 132.00, 131.31, 128.84, 125.20, 123.71, 122.98, 119.06, 118.49, 117.24, 114.41, 113.67, 106.13, 94.26, 93.43, 87.02, 86.26, 80.96, 74.02, 73.47, 71.31, 70.84, 69.23, 32.05, 30.48, 29.87, 29.82, 29.77, 29.56, 29.49, 26.25, 22.85, 22.81, 20.94, 13.97, 10.45; MS (MALDI-TOF) m/z 4287.7 [M + Ag$^+$]; $C_{282}H_{404}O_{24}$ (4178.35).

Acknowledgment. Financial support by the VW-Stiftung for a part of this work is gratefully acknowledged. We also thank Professor P. Bäuerle for access to the STM.

Supporting Information Available: Synthetic schemes for diiodophenol, ^{1}H NMR spectra for **13** and **1a**, texture of the metastable LC-phase of **1b**, NMR dilution experiments for **1c** in CD_2Cl_2/hexanes (1:3) and CD_2Cl_2/hexanes (1:6), energy-minimized structures and energetic parameters of the macrocyclic ring, additional calculated potential curves of the macrocyclic ring in the presence of HOPG (PDF). This material is available free of charge via the Internet at http://pubs.acs.org.

JA003990X